

## RESEARCH ARTICLE

# The relationship between intracellular and plasma levels of folate and metabolites in the methionine cycle: A model

Tanya M. Duncan<sup>1</sup>, Michael C. Reed<sup>2</sup> and H. Frederik Nijhout<sup>1</sup>

<sup>1</sup>Department of Biology, Duke University, Durham, NC, USA

<sup>2</sup>Department of Mathematics, Duke University, Durham, NC, USA

**Scope:** Folate status and the status of the methionine cycle are typically assessed by measuring folate and metabolites in the plasma. It is assumed that plasma metabolite levels are proportional to their levels in tissues, but there is little information to support this assumption.

**Methods and results:** We developed a mathematical model, based on known kinetics of the methionine cycle in the liver and tissues, and the transport kinetics of metabolites into and out of the plasma. We use the model to explore the relationship between folate status and metabolite values in the plasma, the relationships between metabolite values and methylation capacity, the response to a methionine load, and the half-life of folate in plasma and tissues. We also use the model to study the effects of Down syndrome and oxidative stress on metabolite values in plasma and tissues. The model accurately reproduces measured metabolite values pre- and post-folate fortification. The model shows that a high acute intake of folate remains largely restricted to the plasma and is rapidly excreted; only a prolonged exposure to increased folate elevates tissue folate significantly.

**Conclusion:** The model accurately reproduces experimental and clinical findings and can serve as a platform to study, *in silico*, the relationships between metabolite values in tissues and plasma, and how these vary with methionine and B vitamin input, and with mutations in the genes for enzymes in the methionine cycle.

## Keywords:

Folate deficiency / Homocysteine / Mathematical model / Methionine cycle / Methylation



Additional supporting information may be found in the online version of this article at the publisher's web-site

Received: February 23, 2012

Revised: July 25, 2012

Accepted: September 10, 2012

## 1 Introduction

The methionine cycle plays a critical role in cell metabolism and defects in methionine metabolism are associated with a variety of diseases ranging from cardiovascular disease to psychiatric disorders, DNA methylation status, and cancer [1–5]. One of the metabolites in the methionine cycle, *S*-adenosylmethionine (SAM), is the universal methyl donor and is the substrate for a host of methyltransferases among which are the DNA methyltransferases and histone

methyltransferases that regulate gene silencing and epigenetic inheritance. The level of SAM varies with methionine input and folate status, and, together with its product *S*-adenosylhomocysteine (SAH), is used as an indicator of methylation capacity [6, 7]. Another metabolite in the methionine cycle is homocysteine, and elevated levels of homocysteine are generally accepted as a major biomarker for cardiovascular disease [8, 9]. In addition, via the cystathionine- $\beta$ -synthase (CBS) reaction, the methionine cycle provides the first step in the synthesis of reduced glutathione, a key antioxidant.

Aberrant function of the methionine cycle can arise from mutations in the genes that code for enzymes in the cycle and from deficiencies in vitamin cofactors for the enzymes. Vitamin B<sub>12</sub> is an essential cofactor for methionine synthase (MS), which accepts methyl groups from 5-methyltetrahydrofolate and remethylates homocysteine to form methionine. Vitamin B<sub>6</sub> is a cofactor for CBS, which transmethylates homocysteine

**Correspondence:** Professor H. Frederik Nijhout, Department of Biology, Duke University, Durham, NC 27708, USA

**E-mail:** hfn@duke.edu

**Abbreviations:** CBS, cystathionine- $\beta$ -synthase; MS, methionine synthase; SAH, *S*-adenosylhomocysteine; SAM, *S*-adenosylmethionine

and removes it from the methionine cycle in the synthesis of cystathionine, the first step in the synthesis of glutathione.

The status of the methionine cycle is typically assessed by measuring the levels of its metabolites and its vitamin cofactors in the plasma. Plasma homocysteine, methionine, SAM, the SAM/SAH ratio, folate, and vitamins B<sub>6</sub> and B<sub>12</sub> are widely used as indicators of folate sufficiency, methylation capacity, and risk for heart disease and cancer. Although plasma metabolites are well established as biomarkers of disease, an understanding of the mechanism of disease requires knowing metabolite levels in the tissues where the methionine cycle operates. Thus, it would be useful to know how the plasma levels of metabolites reflect their corresponding status within tissues. Unfortunately, it is difficult to obtain simultaneous plasma and tissue measurements for many metabolites over time, in different genetic backgrounds, and under various nutrient and micronutrient inputs.

Because much is known about the kinetics of the methionine cycle and the transport kinetics of metabolites into and out of the tissue and plasma compartments, it is possible to develop a mathematical model that allows us to examine, *in silico*, the expected association between tissue and plasma metabolite levels under many different genetic and environmental conditions. Here, we report on the development of such a model that is based on previous models of the methionine cycle in the liver and in peripheral tissues into which we have incorporated a plasma compartment and in which we can account for dietary input of methionine and folate, their metabolism inside cells, the transport of metabolites between compartments and their elimination in the urine. We show that this model correctly reproduces a variety of experimental and clinical data, and we use the model to show that under certain conditions plasma levels of metabolites can be poor indicators of their corresponding levels in the tissues.

## 2 Methods

We developed a mathematical model for intracellular methionine cycle kinetics, input of substrates into the plasma, transport of metabolites between cells and the plasma, and removal of metabolites by catabolism and excretion. The model has three compartments: plasma, liver, and peripheral tissues. The metabolic reaction diagrams and transport directions are shown in Fig. 1. The kinetics of the liver and tissue methionine cycle are derived from [10] and [11], respectively. The model consists of 16 differential equations that express the rates of change of the metabolites in Fig. 1. Each of the differential equations is a mass balance equation; the time rate of change of the particular metabolite equals the sum of the rates at which it is being made minus the rates it is being consumed in biochemical reactions, plus or minus the net transport rates from or to other compartments. The differential equations, rate equations, transporter kinetics, and justifications are explained in detail in “Supporting Information” together with all parameter values and steady-state values. The model was implemented in MATLAB (Mathworks, Natick, MA, USA).

## 3 Results and discussion

### 3.1 Meaning of the compartments

The model we have developed consists of three compartments: the liver, peripheral tissues, and plasma (Fig. 1). Input of methionine and folate is transferred to the plasma compartment and from there to the liver and peripheral tissues. The peripheral tissue compartment represents all metabolizing tissues in the body, including the kidney. The excretory

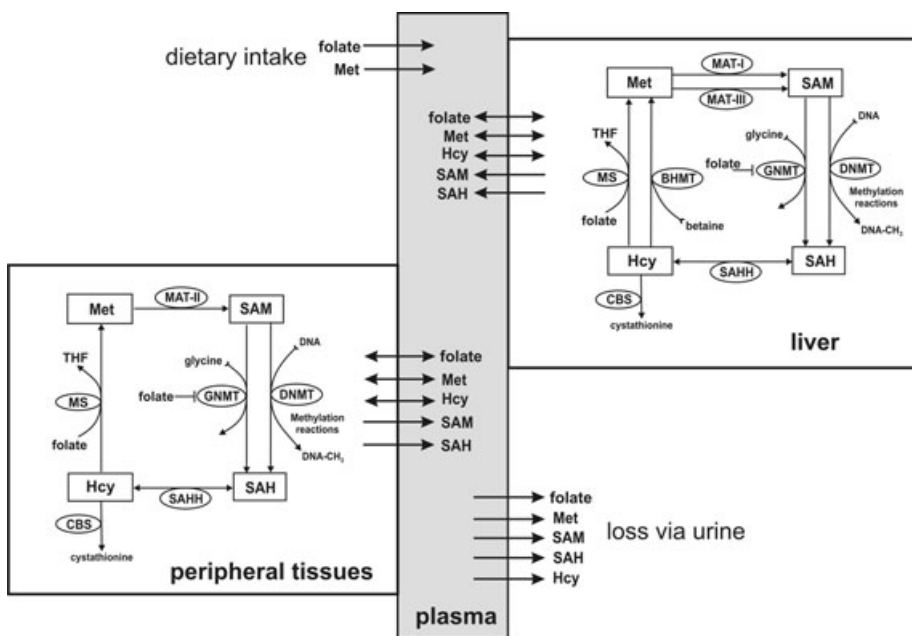


**Figure 1.** The compartment model. Plasma metabolites are affected by dietary input, urinary output, metabolism, and transport into and out of metabolizing tissues.

**Table 1.** Concentration of metabolites at steady state (prefortification)

Metabolite	[Plasma]	[Liver]	[Tissue]
Folate	12.40 nM	9.06 $\mu$ M	0.416 $\mu$ M
Met	33.80 $\mu$ M	88.10 $\mu$ M	54.80 $\mu$ M
SAM	91.42 nM	84.80 $\mu$ M	29.40 $\mu$ M
SAH	24.50 nM	14.10 $\mu$ M	5.02 $\mu$ M
Hcy	8.78 $\mu$ M	3.28 $\mu$ M	1.04 $\mu$ M

role of the kidney is represented by direct output from the plasma compartment. We recognize that no two tissues are likely to have identical metabolite levels or transport rates, so our tissue compartment represents an average effect, which in many cases may correspond to that found in red blood cells.

### 3.2 The steady state

The steady-state values of metabolite concentrations computed by the model for the liver, plasma, and tissues are shown in Table 1. The input and output rates and the net intercompartment flux rates are in Table 2. These model steady-state concentrations and flux rates are within the normal or control ranges reported in the experimental and clinical literature (see Supporting Information). In the model, we can alter the input rates of methionine and folate, we can model the effects of under- and over-expression of the transporters and the enzymes in the methionine cycle, and we can account for the effects of changes in availability of vitamins B<sub>6</sub> and B<sub>12</sub> insofar as they affect the activities of the CBS and MS reactions, respectively, by altering the  $V_{\max}$  of those reactions.

For each of these changes, alone or in combination, we can compute the effects on tissue and plasma concentrations of metabolites and intercompartment fluxes at steady state. In addition, we can compute how concentrations and fluxes will change dynamically over time with varying inputs. In the sections that follow we use the model to simulate various experimental and clinical findings.

### 3.3 Folate: Pre- and postfortification

NHANES data from 1988 to 1994 indicated that the average folate intake was 200  $\mu$ g/day. After the implementation of

**Table 3.** Effect of folate fortification on folate and homocysteine levels

Metabolite	<i>n</i>	NHANES <sup>a),b)</sup>	Model
Plasma folate <sup>c)</sup>			
Prefortification (1988–1994)	9990	12.1 $\pm$ 0.3	12.4
Postfortification (1999–2000)	3223	30.2 $\pm$ 0.7	18.8
Postfortification (2001–2002)	3931	27.8 $\pm$ 0.5	
Tissue folate <sup>c)</sup>			
Prefortification (1988–1994)	9987	391 $\pm$ 0.5	416
Postfortification (1999–2000)	3249	618 $\pm$ 0.11	622
Postfortification (2001–2002)	3977	611 $\pm$ 0.9	
Plasma Hcy <sup>d)</sup>			
Prefortification (1988–1994)	4193	8.7 $\pm$ 0.01	8.7
Postfortification (1999–2000)	3246	7.0 $\pm$ 0.01	6.5
Postfortification (2001–2002)	3976	7.3 $\pm$ 0.01	

a) NHANES analysis from [13].

b) Values are geometric means  $\pm$  SE.

c) nmol/L.

d)  $\mu$ mol/L.

folate fortification in the United States by the FDA in 1998, the average folate intake increased to 300  $\mu$ g/day [12]. Our model assumes that the daily intake of folate is at prefortification levels (200  $\mu$ g/day) and we simulated postfortification levels of 300  $\mu$ g/day regime by increasing folate input in our model by 50%. Our results are shown in Table 3, together with NHANES pre- and postfortification data [13]. The model predicts folate and homocysteine levels within the ranges of the NHANES data for tissue folate as well as plasma Hcy levels with the exception of plasma folate levels postfortification, where NHANES found a higher level than our model suggests. Plasma folate levels are very sensitive to recent folate intake [14], and are thus quite variable, and this may account for the discrepancy. Our model shows that to obtain the NHANES postfortification plasma folate concentration shown in Table 3 would require an intake of 400  $\mu$ g/day, which is only 100  $\mu$ g/day above our assumption and could be achieved by taking a 1/4 of a typical daily multivitamin pill.

We simulated the steady-state effects of a broad range of variation in folate input. The dose–response curves for various metabolites in relation to plasma folate are shown in Fig. 2. The range of values spans the pre- and post-fortified levels of plasma folate (gray lines in Fig. 2). The highest levels of plasma folate shown in Fig. 2 were obtained by

**Table 2.** Metabolite input, removal, and compartment transport rates ( $\mu$ M/h)<sup>a)</sup>

Metabolite	Dietary intake	Flux plasma to liver	Flux plasma to tissue	Net excretion rate	Liver catabolism	Tissue catabolism
Folate	0.0024	0.0015	0.0008	0.0001	0.0015	0.0008
Methionine	106	65.75	38.56	1.69	.	.
Hcy	.	3.77	–3.91	0.14	.	.
SAM	.	–0.05	–0.77	0.82	.	.
SAH	.	–0.008	–0.026	0.034	.	.

a) Net intercompartment flux rates. A negative symbol indicates transport toward the plasma.

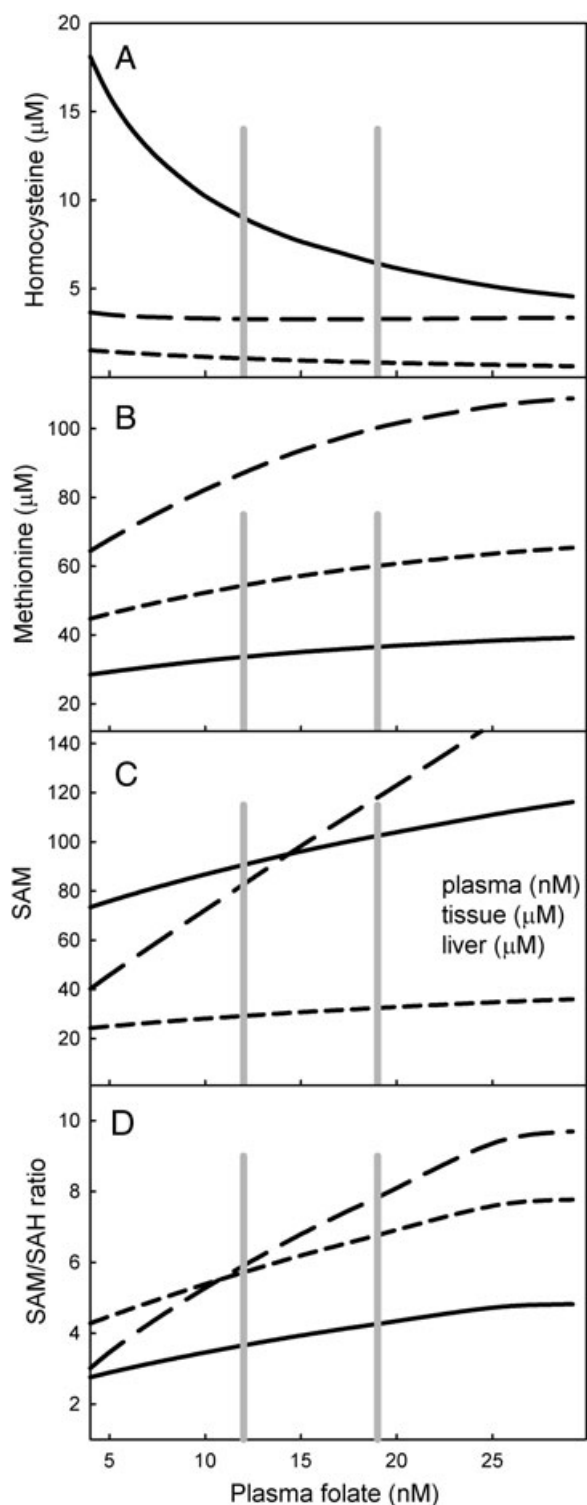


**Figure 2.** Relationships between steady-state plasma folate levels and various metabolite levels due to variation in folate input. (A) homocysteine; (B) methionine; (C) SAM; (D) SAM/SAH ratio. Solid lines represent plasma, long dashes are liver, short dashes are tissue. Vertical gray lines indicate plasma folate levels calculated with the model from pre- and postfortification folate intake levels.

simulating the recommended dietary folate intake of 400  $\mu\text{g}/\text{day}$ . The level of plasma homocysteine is inversely proportional to plasma folate level (Fig. 2A), and corresponds well to the relationship found by [15]. Our model suggests that tissue and liver homocysteine levels vary much less with variation in folate. The concentrations of SAM, the universal methyl group donor, show a different pattern (Fig. 2C). The liver content of SAM is quite sensitive to folate diminution whereas the levels of tissue and plasma SAM change much less with declining folate status.

We examined the effect of variation of folate status on the relationship between the SAM/SAH ratio and the rate of the DNA-methyltransferase (DNMT) reaction (Fig. 3A). Our model uses the kinetics of DNMT-1, the maintenance methyltransferase, which is the principal methyltransferase active in

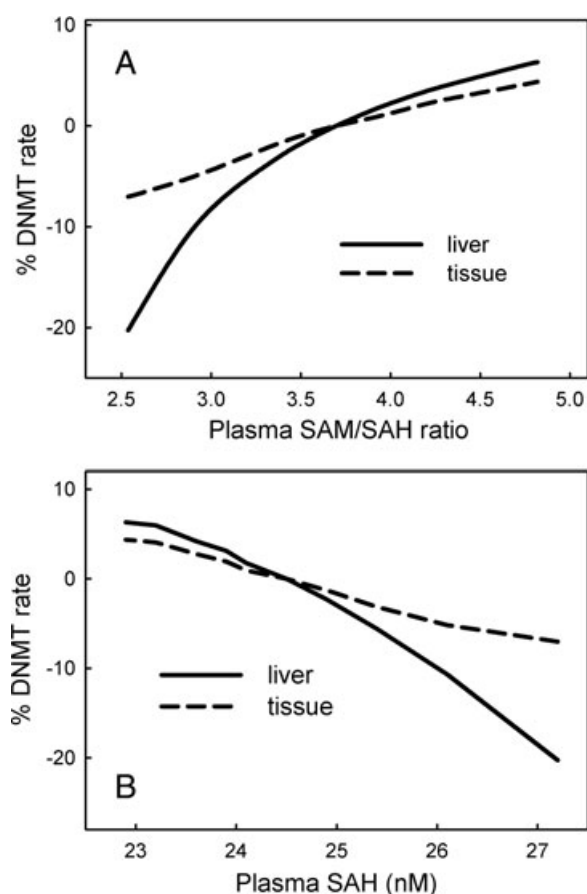


**Figure 3.** Rate of the DNMT reaction in relation to plasma metabolite levels. The DNMT reaction represents methylation capacity. (A) Relationship between SAM/SAH ratio and methylation capacity in liver and peripheral tissue as both vary with folate status. The plasma SAM/SAH ratio at normal folate status is computed by the model as 3.4, which is within the range found experimentally [38]. (B) Relationship between plasma SAH level and tissue DNMT rate as both vary with folate input. Plasma SAH at normal folate status is computed by the model to be 24.50 nM, which is within the range found experimentally [38].

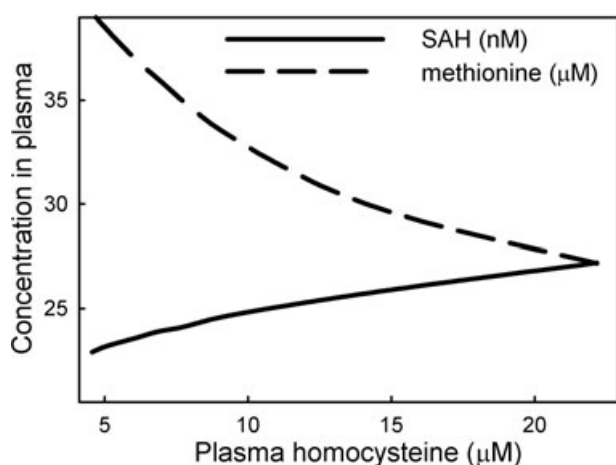


**Figure 4.** Relationship between plasma homocysteine, SAH, and methionine due to variation in folate status. Plasma homocysteine at normal folate status is 12.40  $\mu\text{M}$ .

children and adults [16]. The SAM/SAH ratio is believed to be an indicator of methylation capacity [7, 17]: an increase in SAM enhances methyl-transfer reactions, and a decrease in SAH enhances methylation because SAH is a general inhibitor of methyltransferases. In our model, we assume that the flux through the DNMT reaction is proportional to the DNA methylations capacity. Figure 3A shows that methylation rate is proportional to the plasma SAM/SAH ratio and that the liver shows a stronger positive relation than the peripheral tissues. Yi et al. [18] found a positive relationship between plasma SAH and DNA hypomethylation. Our simulation data likewise show a severe decline in flux through DNMT with increasing plasma SAH level (Fig. 3B). Yi et al. [18] also found a positive relationship between plasma homocysteine and plasma SAH, and a negative relationship between plasma homocysteine and plasma methionine in healthy women with small variation in plasma homocysteine (5–17  $\mu\text{M}$ ). We likewise found a positive relationship of plasma homocysteine with plasma SAH and a negative relationship with plasma methionine (Fig. 4).

### 3.4 Folate half-life and excess folate dosing

In order to verify that in our model net folate elimination and decay kinetics corresponded to observed values, we measured the half-life of folate by setting folate input to zero and following the folate concentrations in the three compartments over time. The decay profiles are shown in Fig. 5. The half-life was 98.5 days, which corresponds well with the approximately 100 days estimates of net folate half-life reported in several studies [19–21]. Because the decay and removal rates of folate are slow relative to the intercompartment folate transport and exchange rates, all compartments remain in mutual equilibrium and the half-life of folate in each compartment is identical (Fig. 5).

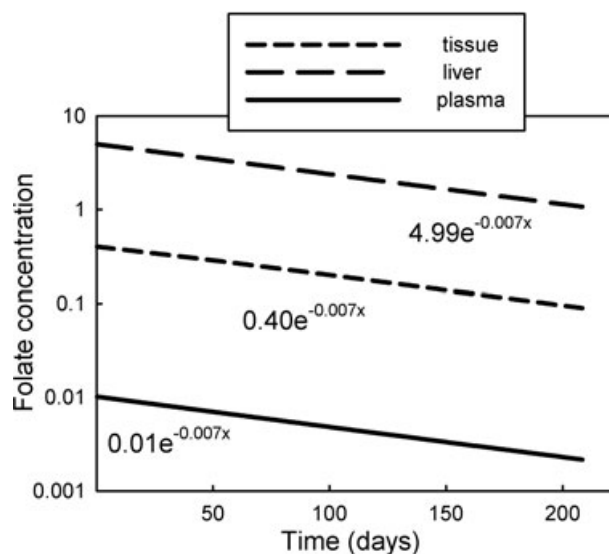


**Figure 5.** Decay of folate in the three compartments after stopping folate input, showing identical half-lives (98.5 days) in each compartment.

Folates bind to and inhibit many enzymes in the folate cycle, a phenomenon known as substrate inhibition [22]. This is a homeostatic mechanism that may be an adaptation to periods of insufficient folate input because, as folate levels decline, enzyme activity increases and this maintains the reaction rates in the folate and methionine cycles [22–24]. There has been concern expressed about the possible deleterious effects of excessive folate intake because increasing folate levels could increase enzyme inhibition and thus have an effect equivalent to a folate deficiency [25–27]. Experimental data, however, suggest that high folate intake has only a modest effect on tissue and plasma folate levels, possibly due to saturable uptake and retention processes [28]. We simulated excessive folate intake in our model and monitored tissue levels and urinary excretion.

When we increased folate input by twofold we saw a rapid rise of plasma folate and a rapid increase in folate excretion during the first 10 h, followed by a much slower rise in plasma folate level and urinary excretion rate (Fig. 6). A persistently high level of plasma folate due to a chronic twofold input leads to a slow but continuous elevation of plasma and intracellular folate, which reach their new steady state at twice the normal level (100% increase) after about 650 days.

We next simulated the fate of a large infusion of excess folate by increasing folate input 100-fold for a period of 2 h and following metabolite profiles for the next 60 h (Fig. 7). The folate remained largely in the plasma before being removed by urinary excretion, and there was a slight but persistent rise in liver and tissue folate (6 and 5%, respectively). Overall, the results of our simulations indicate that a brief excessive dietary folate input remains largely restricted to the plasma and is rapidly eliminated. It causes only a small rise in tissue

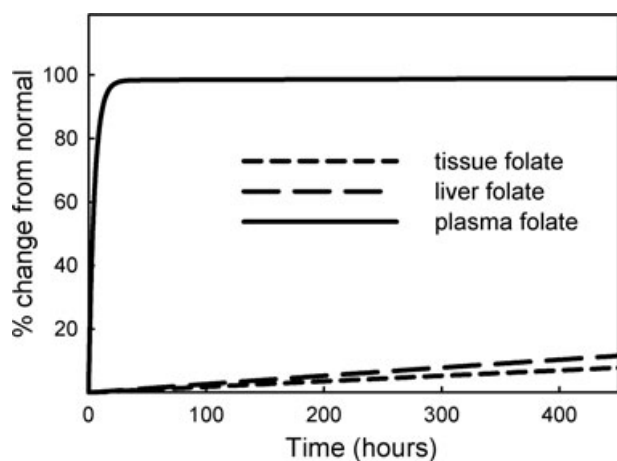


**Figure 6.** Simulation of a chronic twofold rate of folate input. At steady-state plasma folate levels off at 25.3 nM (normal = 12.40 nM), liver folate at 18.1  $\mu$ M (normal = 9.06  $\mu$ M), and tissue folate at 0.83  $\mu$ M (normal = 0.416  $\mu$ M).

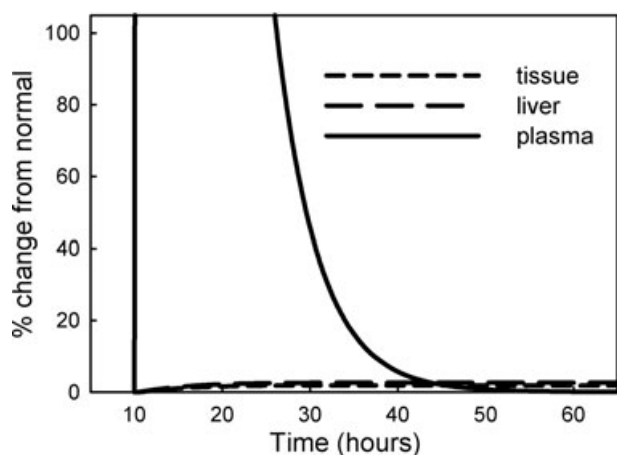


**Figure 7.** Simulation of an acute folate load. An infusion of 100-fold normal folate input for 2 h, starting at 10 h, causes a large rise in plasma folate and a small but persistent elevation of intracellular folate.

folate; this elevated tissue folate declines very slowly and takes some 800 days to return to normal.

### 3.5 Vitamin B<sub>12</sub> deficiency

Vitamin B<sub>12</sub> is a necessary cofactor for MS, the enzyme that remethylates homocysteine to methionine using a methyl group from 5-methyltetrahydrofolate. We modeled the effect of a vitamin B<sub>12</sub> deficiency by reducing the  $V_{max}$  of the MS reactions in tissue and liver by 20%. Table 4 shows the results of this simulation in the context of pre- and postfortification folate input levels. Our model accurately reproduced plasma homocysteine levels from the NHANES study analyzed by Selhub et al. [29]. Lowered levels of vitamin B<sub>12</sub> were associ-

**Table 4.** Plasma homocysteine levels ( $\mu$ mol/L) in response to variation in folate and vitamin B<sub>12</sub> levels

Folate level <sup>(a)</sup>	Low B <sub>12</sub> (80%) <sup>(c)</sup>	High B <sub>12</sub> (100%)
Low		
Model	12.52	8.78
NHANES <sup>(b)</sup>	11.9–15.5	7.6–10.9
High		
Model	8.85	6.48
NHANES <sup>(b)</sup>	9.9–11.8	7.1–9.2

a) Low and high levels of folate in the model correspond to mean pre- and postfortification input levels.

b) Range of least-squares geometric means of plasma Hcy calculated from pre- and postfortification NHANES data from [29].

c) The effect of a B<sub>12</sub> deficiency was modeled by reducing the  $V_{max}$  of the methionine synthase reactions in liver and tissue to 80%.

ated with elevated plasma homocysteine, and this effect was completely reversed by the higher postfortification level of folate intake. In our model, a B<sub>12</sub> deficiency also causes an accumulation of folate as 5-methyltetrahydrofolate, in accord with the “methyl-trap” hypothesis [24, 30]. One concern with folate fortification is that it can mask a B<sub>12</sub> deficiency. We therefore modeled the effect of variation in B<sub>12</sub> status with variation in folate intake (Fig. 8). These response surfaces illustrate that the relationships are nonlinear and the relative effects of variation in folate and B<sub>12</sub> depend on the amount of variation and on where exactly on the surface an individual is located.

### 3.6 Methionine load

Methionine loading is used as a test for deficiency in transmethylation of homocysteine, which could be due to functional mutations in the gene for CBS, or a reduced vitamin B<sub>6</sub> status. We simulated methionine loading by introducing a 2-h methionine pulse at six times the normal input rate. The methionine pulse appears in the plasma as a peak that resolves in 10–15 h. Homocysteine in the plasma rises gradually to just above 30  $\mu$ M, (four times above basal level) and declined to near basal level 24–30 h after initiation of the methionine pulse (Fig. 9), as found experimentally in [31, 32]. We then reduced CBS activity to 50% of normal and found that a methionine load raised the peak plasma homocysteine level to just over 50  $\mu$ M. Although this looks like an increased response, it is actually only 2.5 times the higher basal level of homocysteine that is characteristic of a CBS deficiency. Silberberg and Dudman [33] noted that homocysteine levels after a methionine load are not always measured relative to the correct basal level of homocysteine, suggesting that reports of elevated homocysteine following a methionine load may not always be reliable. In the mathematical model presented here the percent increase relative to baseline is similar whether or not there is a CBS deficiency. Guttormsen

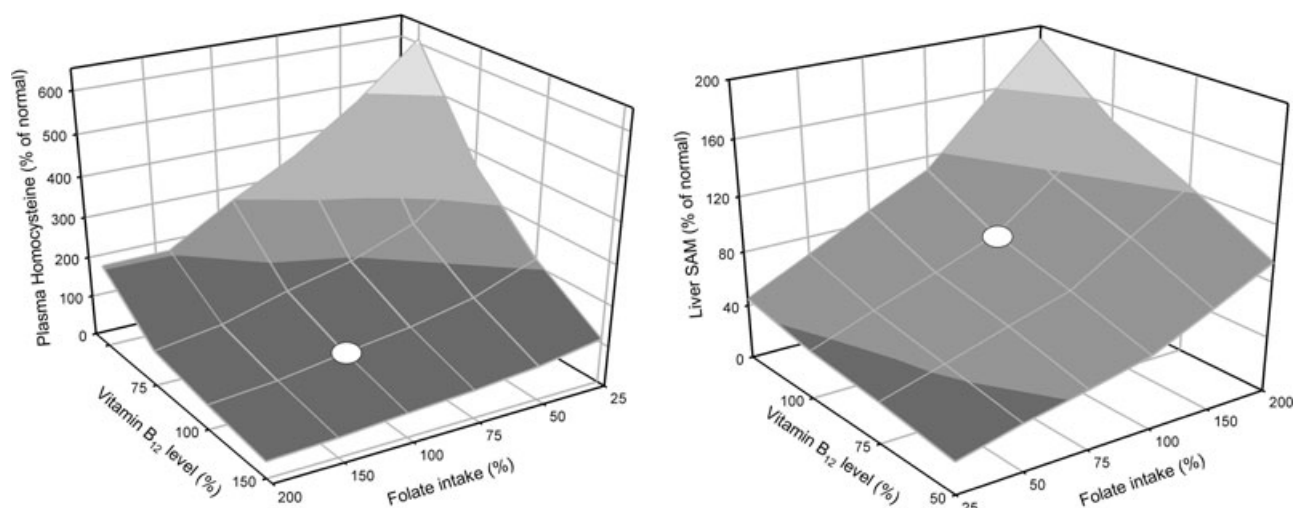


**Figure 8.** Simulation of effect of simultaneous variation in folate intake and vitamin B<sub>12</sub> status on plasma homocysteine and liver SAM. Values represent percent of normal. For folate normal is the prefortification intake. Variation in vitamin B<sub>12</sub> was modeled by varying the  $V_{\max}$  of methionine synthase in liver and tissue. White dots indicate prefortification values of folate intake and normal vitamin B<sub>12</sub> status.

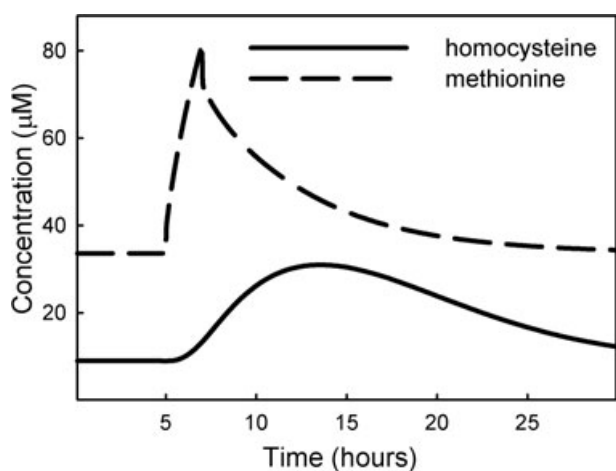


**Figure 9.** Simulation of methionine load. Methionine input was raised sixfold for a 2-h period, starting at 5 h.

et al. [34] measured the half-life of intravenously injected homocysteine and found values ranging from 2.8 to 5.2 h. When we raised the initial value of plasma homocysteine twofold, we calculated a half-life of 5.2 h as the concentration returned to steady state, indicating that the homocysteine redistribution kinetics in our model closely resemble those found experimentally.

### 3.7 Down syndrome and oxidative stress

Down syndrome is a complex set of developmental abnormalities that result from trisomy of chromosome 21 [35]. The gene for CBS is on chromosome 21, so some of the symptoms of Down syndrome could be due to over-expression of

CBS [36, 37]. Increased CBS activity will lower the steady-state levels of homocysteine and SAM, which can be interpreted, respectively, as a beneficial and a deleterious effect. In addition, persons with Down syndrome often experience excess oxidative stress [6, 38], which affects the activities of several enzymes in the methionine cycle [10]. We simulated a triple dose of CBS by increasing the  $V_{\max}$  of the enzyme to 150%. We found that homocysteine was depressed by 38% of normal (Table 5), which closely corresponds to that found in persons with Down syndrome [37]. Additionally, SAM decreased which corresponds with the trend found in persons with Down syndrome. The gene for superoxide dismutase is also on chromosome 21, and persons with Down syndrome often suffer from a mild degree of oxidative stress. When we simulated the addition of oxidative stress, we found that homocysteine rose slightly and SAM levels were reduced even more. The decrease in SAM levels corresponds with experimental data [37, 39]. In addition, Infantino et al. [39] found that the levels of methionine were significantly reduced in

**Table 5.** Effect of increasing oxidative stress on homocysteine and SAM concentrations in CBS trisomy

Metabolite	Normal		Down		
	Data <sup>a)</sup>	Model	Data <sup>a)</sup>	Model	Model + 2 H <sub>2</sub> O <sub>2</sub>
Plasma Hcy <sup>c)</sup>	6.7	6.48	4.2	4.1	5.49
Plasma SAM <sup>b)</sup>	98	102.2	65.4	94.2	78.5
Liver Hcy <sup>c)</sup>		3.29		2.15	1.73
Liver SAM <sup>c)</sup>		97.1		91.68	61.24

a) Experimental data from [37].

b) nmol/L.

c) µmol/L.

cultured lymphoblast cells in Down patients. Our model likewise shows a modest decrease in methionine in patients with CBS trisomy which is greatly enhanced by oxidative stress.

#### 4 Concluding remarks

We have developed a mathematical model of methionine metabolism and folate and the transport of metabolites between the plasma, liver, and peripheral tissues for the purpose of investigating, *in silico*, the degree to which metabolite levels that are typically measured in the plasma reflect the levels of their counterparts in the tissues. With this model, we can study the effects of variation in methionine and folate input, as well as variation in the activities of enzymes in the methionine cycle, where variation can be due to mutation, expression level, or availability of vitamin cofactors.

Collection of a blood sample is relatively noninvasive and is a preferred method for assessing health status by measuring the levels of metabolites and drawing inferences from the observed values. The interpretation of the significance of blood values is calibrated by deviations from the typical range and reasonable physiological expectations of functionality. Linkage of a particular range of values with health or disease is derived from statistical association studies. Our model allows us to infer liver and tissue values of metabolites and thus helps us to understand the cellular metabolic mechanisms that cause the changes in plasma levels.

We used the model to study the effect of folate fortification on tissue and plasma homocysteine levels and show a good correspondence to the empirical findings of the NHANES studies. We used the model to calculate the half-life of folate, and found it to be 98 days, which corresponds well with experimental estimates. High doses of folate remained largely in the plasma compartment and were rapidly eliminated via the urine. Although plasma folate rose to high levels, only a small fraction of the plasma folate entered tissues; however, once taken up, the elevated tissue levels persisted for a long time.

We studied the effects of variation in folate intake on the tissue and plasma concentrations of homocysteine, methionine, SAM, and the SAM/SAH ratio (Figs. 2–4). With the exception of methionine, the plasma values do not accurately reflect tissue values. Liver SAM levels increase more severely than plasma SAM levels at high folate status, and this likewise increases the liver SAM/SAH ratio more than is reflected in the plasma. Interestingly, plasma homocysteine levels increased strongly with decreasing folate status, whereas tissue homocysteine levels were much less affected (Fig. 2), suggesting that plasma homocysteine is a hypersensitive indicator of tissue homocysteine levels at lowered folate status.

In our model, methylation capacity is represented by the flux carried by the DNMT reaction. This flux is affected by the concentration of its substrate, SAM, its inhibitor SAH, and by folate status. In accord with experimental findings, our

model showed a positive relationship between the SAM/SAH ratio in the plasma and flux through DNMT, and a negative relationship between plasma SAH levels and flux through DNMT.

We also used the model to simulate the effect of the higher level of CBS activity that occurs in Down syndrome. By itself, the increased CBS activity lowers plasma SAM and plasma homocysteine, as expected. However, some Down patients have an elevated plasma homocysteine, and also suffer from excessive oxidative stress. Oxidative stress affects the activity of several enzymes in the methionine cycle, and previous model results have shown that increased oxidative stress increased hepatic levels of homocysteine [10]. With the present model we were able to show that plasma homocysteine levels also increase with oxidative stress, and that liver and plasma SAM levels decrease.

*This research was supported by NSF grant EF-1038593 to H. F. N. and M. C. R., and a subcontract on NIH grant R01 ES019876 (D. Thomas, PI). We are grateful to Cornelia Ulrich, Jesse Gregory, Barry Shane, and Jill James for helpful discussions.*

*The authors have declared no conflict of interest.*

#### 5 References

- [1] Davis, C., Uthus, E., DNA methylation, cancer susceptibility, and nutrient interactions. *Exp. Biol. Med.* 2004, 229(10), 988–995.
- [2] Gavin, D., Sharma, R., Histone modifications, DNA methylation, and schizophrenia. *Neurosci. Biobehav. Rev.* 2010, 34(6), 882–888.
- [3] Ma, J., Stampfer, M., Christensen, B., Giovannucci, E. et al., A polymorphism of the methionine synthase gene: association with plasma folate, vitamin B12, homocyst(e)ine, and colorectal cancer risk. *Cancer Epidemiology Biomarkers Prev.* 1999, 8(9), 825–829.
- [4] Refsum, H., Ueland, P., Nygard, O., Vollset, S., Homocysteine and cardiovascular disease. *Ann. Rev. Med.* 1998, 49, 31–62.
- [5] Sharma, A., Kramer, M., Wick, P., Liu, D. et al., D4 dopamine receptor-mediated phospholipid methylation and its implications for mental illnesses such as schizophrenia. *Mol. Psychiatry* 1999, 4, 235–246.
- [6] James, S., Cutler, P., Melnyk, S., Jernigan, S. et al., Metabolic biomarkers of increased oxidative stress and impaired methylation capacity in children with autism. *Am. J. Clin. Nutr.* 2004, 80(6), 1611–1617.
- [7] Caudill, M., Wang, J., Melnyk, S., Pogribny, I. et al., Intracellular S-adenosylhomocysteine concentrations predict global DNA hypomethylation in tissues of methyl-deficient cystathionine  $\beta$ -synthase heterozygous mice. *J. Nutr.* 2001, 131, 2811–2818.
- [8] Selhub, J., Homocysteine metabolism. *Annu. Rev. Nutr.* 1999, 19, 217–246.

- [9] Wald, D., Law, M., Morris, J., Homocysteine and cardiovascular disease: evidence on causality from a meta-analysis. *Br. Med. J.* 2002, *325*, 1–7.
- [10] Reed, M., Thomas, R., Paviscic, J., James, S. et al., A mathematical model of glutathione metabolism. *Theor. Biol. Med. Model.* 2008, *5*, 8.
- [11] Ulrich, C., Neuhouser, M., Liu, A., Boynton, A. et al., Mathematical modeling of folate metabolism: predicted effects of genetic polymorphisms on mechanisms and biomarkers relevant to carcinogenesis. *Cancer Epidemiology Biomarkers Prev.* 2008, *17*, 1822–1831.
- [12] Bentley, T. G. K., Willett, W. C., Weinstein, M. C., Kuntz, K. M., Population-level changes in folate intake by age, gender, and race/ethnicity after folic acid fortification. *Am. J. Public Health* 2006, *96*, 2040–2047.
- [13] Ganji, V., Kafai, M. R., Trends in serum folate, RBC folate, and circulating total homocysteine concentrations in the United States: analysis of data from National Health and Nutrition Examination Surveys, 1988–1994, 1999–2000, and 2001–2002. *J. Nutr.* 2006, *136*, 153–158.
- [14] Lindenbaum, J., Allen, R., In: Bailey, L. B. (Ed.), *Folate in Health and Disease*, Marcel Dekker, Inc. New York 1995, pp. 43–66.
- [15] Selhub, J., Jacques, P., Wilson, P., Rush, D. et al., Vitamin status and intake as primary determinants of homocysteinemia in an elderly population. *JAMA* 1993, *270*, 2693–2698.
- [16] Pradhan, S., Esteve, P., Mammalian DNA (cytosine-5) methyltransferases and their expression. *Clin. Immunol.* 2003, *109*, 6–16.
- [17] Williams, K., Schalinske, K., New insights into the regulation of methyl group and homocysteine metabolism. *J. Nutr.* 2007, *137*, 311–314.
- [18] Yi, P., Melnyk, S., Pogribna, M., Pogribny, I. et al., Increase in plasma homocysteine associated with parallel increases in plasma S-adenosylhomocysteine and lymphocyte DNA hypomethylation. *J. Biol. Chem.* 2000, *275*, 29318–29323.
- [19] Gregory, J., Quinlivan, E., In vivo kinetics of folate metabolism. *Annu. Rev. Nutr.* 2002, *22*, 199–220.
- [20] Gregory, J., Scott, K., Modeling of folate metabolism. *Adv. Food Nutr. Res.* 1996, *40*, 81–93.
- [21] Stites, T., Bailey, L., Scott, K., Toth, J. et al., Kinetic modeling of folate metabolism through use of chronic administration of deuterium-labeled folic acid in men. *Am. J. Clin. Nutr.* 1997, *65*, 53–60.
- [22] Reed, M. C., Lieb, A., Nijhout, H. F., The biological significance of substrate inhibition: a mechanism with diverse functions. *Bioessays* 2010, *32*, 422–429.
- [23] Nijhout, H. F., Reed, M. C., Anderson, D., Mattingly, J. et al., Long-range allosteric interactions between the folate and methionine cycles stabilize DNA methylation reaction rate. *Epigenetics* 2006, *1*, 81–87.
- [24] Nijhout, H. F., Reed, M. C., Budu, P., Ulrich, C., A mathematical model of the folate cycle. *J. Biol. Chem.* 2004, *279*, 55008–55016.
- [25] Troen, A., Mitchell, B., Sorensen, B., Wener, M. et al., Unmetabolized folic acid in plasma is associated with reduced natural killer cell cytotoxicity among postmenopausal women. *J. Nutr.* 2006, *136*, 189–194.
- [26] Ulrich, C., Potter, J., Folate supplementation: too much of a good thing? *Cancer Epidemiology Biomarkers Prev.* 2006, *15*, 189–193.
- [27] Smith, A., Kim, Y-I, Refsum, H., Is folic acid good for everyone? *Am. J. Clin. Nutr.* 2008, *87*(3), 517–533.
- [28] Gregory, J., Williamson, J., Bailey, L., Toth, J., Urinary excretion of [2H4]folate by nonpregnant women following a single oral dose of [2H4]folic acid is a functional index of folate nutritional status. *J. Nutr.* 1998, *128*, 1907–1912.
- [29] Selhub, J., Morris, M., Jacques, P., In vitamin B-12 deficiency, higher serum folate is associated with increased total homocysteine and methylmalonic acid concentrations. *Proc. Natl. Acad. Sci. USA* 2007, *104*, 19995–20000.
- [30] Shane, B., In: Bailey, L. B. (Ed.), *Folate in Health and Disease*, Marcel Dekker, Inc., New York 1995, pp. 1–22.
- [31] Loehrer, F., Haefli, W., Angst, C., Browne, G. et al., Effect of methionine loading on 5-methyltetrahydrofolate, S-adenosylmethionine and S-adenosylhomocysteine in plasma of health humans. *Clin. Sci.* 1996, *91*, 79–86.
- [32] Ueland, P., Refsum, H., Plasma homocysteine, a risk factor for vascular disease: plasma levels in health, disease, and drug therapy. *J. Lab. Clin. Med.* 1989, *114*, 473–501.
- [33] Silberberg, J., Dudman, N., In: Carmel, R., Jacobsen, D. (Eds.), *Homocysteine in Health and Disease*, Cambridge University Press, Cambridge 2001, pp. 212–219.
- [34] Guttormsen, A., Mansoor, A., Fiskerstrand, T., Ueland, P. et al., Kinetics of plasma homocysteine in healthy subjects after peroral homocysteine loading. *Clin. Chem.* 1993, *39*, 1390–1397.
- [35] Epstein, C. J., In: Stanbury, J. B., Wingarden, J. B., Frederickson, D. F. (Eds.), *The Metabolic and Molecular Bases of Inherited Disease*, 3rd edition, McGraw-Hill, New York 1995, pp. 749–794.
- [36] Pogribna, M., Melnyk, S., Pogribny, I., Chango, A. et al., Homocysteine metabolism in children with Down syndrome: in vitro modulation. *Am. J. Hum. Genet.* 2001, *69*, 88–95.
- [37] Al-Gazali, L. I., Padmanabhan, R., Melnyk, S., Yi, P. et al., Abnormal folate metabolism and genetic polymorphism of the folate pathway in a child with Down syndrome and neural tube defect. *Am. J. Med. Genet.* 2001, *103*, 128–132.
- [38] Melnyk, S., Pogribna, M., Pogribny, I., Yi, P. et al., Measurement of plasma and intracellular S-adenosylmethionine and S-adenosylhomocysteine utilizing coulometric electrochemical detection: alterations with plasma homocysteine and pyridoxal 5'-phosphate concentrations. *Clin. Chem.* 2000, *46*, 265–272.
- [39] Infantino, V., Castegna, A., Iacobazzi, F., Spera, I. et al., Impairment of methyl cycle affects mitochondrial methyl availability and glutathione level in Down's syndrome. *Mol. Genet. Metab.* 2011, *102*, 378–382.

## The relationship between intracellular and plasma levels of folate and metabolites in the methionine cycle: A model

Tanya M. Duncan<sup>1</sup>, Michael. C. Reed<sup>2</sup> and H. Frederik Nijhout<sup>1,3</sup>

<sup>1</sup>Department of Biology, <sup>2</sup>Department of Mathematics, Duke University, Durham, NC 27708

<sup>3</sup>Corresponding author: e-mail hfn@duke.edu

Address: <sup>1</sup>Department of Biology, Duke University, Durham, NC 27708, <sup>2</sup>Department of Mathematics, Duke University, Durham, NC 27708

### Model Diagram

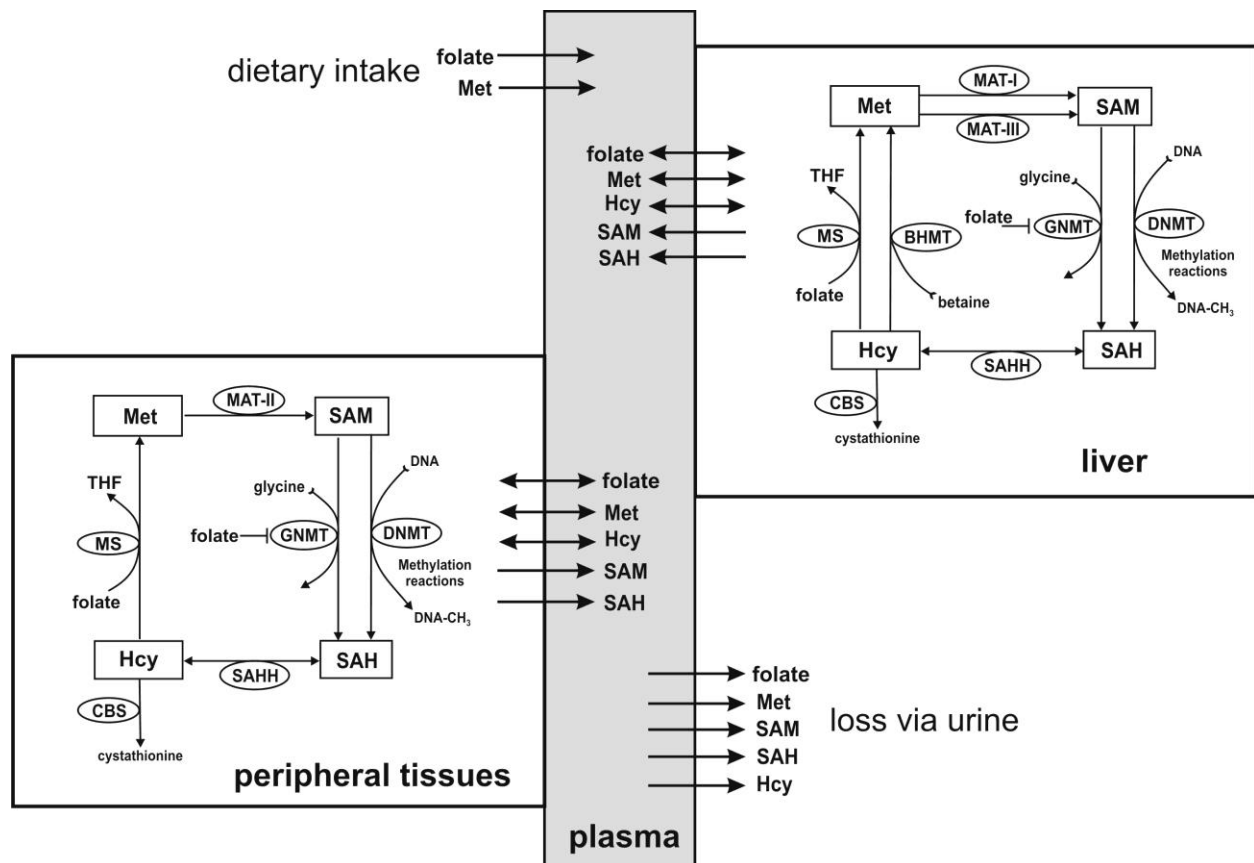


Figure 1. Reaction diagram of the three-compartment model

## Model Details

The model consists of 16 differential equations that express the rates of change of the metabolites in Figure 1. Each of the differential equations is a mass balance equation; the time rate of change of the particular metabolite equals the sum of the rates at which it is being made minus the rates it is being consumed in biochemical reactions, plus or minus the net transport rates from or to other compartments. In order to display the differential equations coherently, we have chosen notation for the variables and reaction rates that is both more uniform and sparse than some notation commonly in use. For example, the concentration of methionine in the liver is denoted lMet instead of the usual [liverMet]. Our notation is described in Part A, below. In Part B, we give the differential equations, which are written in terms of reaction, transport and removal rates, and contain terms to account for the relative sizes of the three compartments. In Part C, the kinetic formulas and constants for these reaction and transport rates are given with justifications. Part D describes metabolite input and removal from the system.

### Part A: Notation.

#### A.1 Names and Acronyms

The names of the enzymes indicated by acronyms in Figure 1 are given in Table S1.

**Table S1: Enzyme names and acronyms**

MAT-I	methionine adenosyl transferase I
MAT-II	methionine adenosyl transferase II
MAT-III	methionine adenosyl transferase III
GNMT	glycine N-methyltransferase
DNMT	DNA-methyltransferase
SAHH	S-adenosylhomocysteine hydrolase
CBS	cystathionine $\beta$ -synthase
MS	methionine synthase
BHMT	betaine-homocysteine methyltransferase

We use three letter acronyms or abbreviations for the metabolites (Table S2). In the equations, these acronyms have a prefix of l, t, p, or u to indicate the compartment, liver, tissue, plasma or urine, respectively.

**Table S2: Names and acronyms of metabolites**

Met	methionine
SAM	S-adenosylmethionine
SAH	S-adenosylhomocysteine
Hcy	homocysteine
Fol	folate

## A.2 Constants

**Table S3: Names and values of constants (concentrations in  $\mu\text{M}$ , time in hours), and size ratios of the three compartments.**

ssH <sub>2</sub> O <sub>2</sub>	0.01	steady state intracellular hydrogen peroxide
H <sub>2</sub> O <sub>2</sub>	0.01	intracellular hydrogen peroxide (varies in some experiments)
Folin	0.0024	hourly input of folate (varies in some experiments)
Metin	106	hourly input of methionine (varies in some experiments)
klp	0.625	liver to plasma size ratio
kpl	1.6	plasma to liver size ratio
ktp	7.5	tissue to plasma size ratio
kpt	0.133	plasma to tissue size ratio

## A.3 Steady State Values

**Table S4: Steady-state values of metabolite concentrations in the liver, plasma and tissues.**

Compartment	Metabolite	Model	Data	Reference
Plasma	Hcy ( $\mu\text{M}$ )	8.78	$8.7 \pm 0.1$	[1]
	SAM (nM)	91.40	35-118	[2]
	SAH (nM)	24.50	9.6-38.7	[2]
	Fol (nM)	12.40	$12.1 \pm 0.3$	[1]
	Met ( $\mu\text{M}$ )	33.80	$24.1 \pm 4.7$	[3]
Liver	Hcy ( $\mu\text{M}$ )	3.28	$3.63 \pm 0.89$	[4]
	SAM ( $\mu\text{M}$ )	84.80	60-90	[4]
	SAH ( $\mu\text{M}$ )	14.10	10-15	[4]
	Fol ( $\mu\text{M}$ )	9.06	9	[5]
	Met ( $\mu\text{M}$ )	88.10	$72.6 \pm 12.5$	[6]
Tissue	Hcy ( $\mu\text{M}$ )	1.04	0.76-1.12	[4]
	SAM ( $\mu\text{M}$ )	29.50	19-50	[4]
	SAH ( $\mu\text{M}$ )	5.02	3.4-6.7	[4]
	Fol (nM)	416	$391 \pm 5.4$	[1]
	Met ( $\mu\text{M}$ )	54.80	$63 \pm 13.0$	[6]

## Part B: The Equations

### B.1 Velocity notation

We denote the velocity of a reaction (in  $\mu\text{M}/\text{hr}$ ) by a capital V, with a subscript indicating the acronym for the enzyme that catalyzes the reaction. For example, the velocity of the methionine synthase (MS) reaction is denoted by  $V_{\text{MS}}$ . For the transport of metabolites into and out of

compartments the velocity and direction of the transport reaction (in  $\mu\text{M/hr}$ ) is indicated by a capital  $V$ , with a subscript indicating the acronym for the metabolite being transported, and the first and last letter surrounding the metabolite indicates its movement. For example, transport of methionine into the liver from the plasma, or out of the liver and into the plasma, are denoted by  $V_{\text{pMetl}}$  and  $V_{\text{lMetp}}$ , respectively.

### ***B.2 Compartment size***

The relative size of each compartment was calculated from the human tissue mass balance data in [7], their Table 21. We calculated the relative size of the plasma, liver, and metabolically active tissue to be 4%, 2.5%, and 30% of the total body mass, respectively. When transferring metabolites from one compartment to the other we multiplied the concentration in the receiving compartment by its size relative to that of the delivering compartment. In the equations, this relative size was expressed as a constant  $k$ , with a subscript with the first letter being the delivering compartment and the second the receiving compartment.

### ***B.3 The differential equations***

$$\frac{d[\text{pHcy}]}{dt} = k_{\text{lp}}V_{\text{lHcyp}} + k_{\text{tp}}V_{\text{tHcyp}} - V_{\text{pHcyl}} - V_{\text{pHcyt}} - V_{\text{pHcy}} + V_{\text{uHcyp}}$$

$$\frac{d[\text{lHcy}]}{dt} = k_{\text{pl}}V_{\text{pHcyl}} - V_{\text{lHcyp}} + V_{\text{SAHH}} - V_{\text{CBS}} - V_{\text{MS}} - V_{\text{BHMT}}$$

$$\frac{d[\text{tHcy}]}{dt} = k_{\text{pt}}V_{\text{pHcyt}} - V_{\text{tHcyp}} + V_{\text{SAHH}} - V_{\text{CBS}} - V_{\text{MS}}$$

$$\frac{d[\text{pSAM}]}{dt} = k_{\text{lp}}V_{\text{lSAMP}} + k_{\text{tp}}V_{\text{tSAMP}} - V_{\text{pSAM}}$$

$$\frac{d[\text{lSAM}]}{dt} = -V_{\text{lSAMP}} + V_{\text{MATI}} + V_{\text{MATIII}} - V_{\text{GNMT}} - V_{\text{DNMT}}$$

$$\frac{d[\text{tSAM}]}{dt} = -V_{\text{tSAMP}} + V_{\text{MATII}} - V_{\text{GNMT}} - V_{\text{DNMT}}$$

$$\frac{d[\text{pSAH}]}{dt} = k_{\text{lp}}V_{\text{lSAHp}} + k_{\text{tp}}V_{\text{tSAHp}} - V_{\text{pSAH}}$$

$$\frac{d[\text{lSAH}]}{dt} = -V_{\text{lSAHp}} + V_{\text{GNMT}} + V_{\text{DNMT}} - V_{\text{SAHH}}$$

$$\frac{d[\text{tSAH}]}{dt} = -V_{\text{tSAHp}} + V_{\text{GNMT}} + V_{\text{DNMT}} - V_{\text{SAHH}}$$

$$\frac{d[\text{pFol}]}{dt} = \text{Folin} - V_{\text{lFolp}} - V_{\text{tFolp}} + V_{\text{tfluxFol}} + V_{\text{lfluxFol}} - V_{\text{pFol}}$$

$$\frac{d[lFol]}{dt} = k_{pl}V_{pFoll} - V_{fluxFol} - V_{lFol}$$

$$\frac{d[tFol]}{dt} = k_{pt}V_{pFolt} - V_{fluxFol} - V_{tFol}$$

$$\frac{d[pMet]}{dt} = Metin + k_{lp}V_{lMetp} + k_{tp}V_{tMetp} - V_{pMetl} - V_{pMett} - V_{pMet}$$

$$\frac{d[lMet]}{dt} = k_{pl}V_{pMetl} - V_{lMetp} + V_{BHMT} + V_{MS} - V_{MATI} - V_{MATIII}$$

$$\frac{d[tMet]}{dt} = k_{pt}V_{pMett} - V_{tMetp} + V_{MS} - V_{MATII}$$

$$\frac{d[uHcy]}{dt} = V_{pHcy} - V_{uHcyp}$$

## Part C. Kinetics

### C.1 Oxidative stress

Intracellular hydrogen peroxide levels ( $H_2O_2$ ) and reduced glutathione (GSSG) play a role in regulating enzyme velocities in the methionine cycle. Hydrogen peroxide inhibits MS and BHMT, and activates CBS [8, 9]. GSSG inhibits MAT I, MAT II, MAT III [10, 11]. To add inhibition by  $H_2O_2$  to our enzyme reactions, we multiplied the reaction velocity by the term

$$\frac{K_i + [H_2O_2]_{ss}}{K_i + [H_2O_2]}$$

where  $K_i$  is the scaling constant, and  $[H_2O_2]_{ss}$  is the concentration at steady-state. Since the inhibitor concentration is in the denominator, the reaction velocity decreases as the concentration of the substrate increases. We chose this format so that the velocity of the reaction at steady-state would remain the same once we added the inhibition. This allows us to compare the system with and without inhibition. We were unable to find kinetic data for the inhibitions by  $H_2O_2$ , so we chose our scaling constants to be the value of steady-state intracellular  $H_2O_2$  concentration so that the effects of the inhibitions would be nearly linear. MAT I, MAT II and MAT III are inhibited indirectly via reduced glutathione (GSSG), which accumulates under oxidative stress. GSSG does not occur in the present model, so we used our model for glutathione synthesis kinetics [12] to calculate the effective scaling constant of  $H_2O_2$  on MAT I and MAT III.

For enzyme activation by  $H_2O_2$ , we used a similar approach. We multiplied the reaction velocity by the term

$$\frac{K_a + [H_2O_2]}{K_a + [H_2O_2]_{ss}}$$

Note that here the activator concentration is in the numerator, and so as the concentration of the substrate increases, so does the velocity of the reaction. Again, the multiplier is one at steady-state, allowing for comparison of the system with and without inhibition.

## C2. Enzyme Kinetic

**MAT-I:** The MAT-I kinetics are from [13], Table 1, and we take  $V_{\max} = 301.2 \mu\text{M/hr}$  and  $K_m = 41$ . The inhibition by SAM was derived by non-linear regression on the data from [13], Figure 5. The last factor represents the inhibition of MAT-I by oxidative stress, with  $K_i=35$ , see the discussion above.

$$V_{\text{MATI}} = (0.23 + 0.8e^{-0.0026[\text{SAM}]}) \left( \frac{V_{\max}[\text{Met}]}{K_m + [\text{Met}]} \right) \left( \frac{K_i + [\text{H}_2\text{O}_2]_{\text{SS}}}{K_i + [\text{H}_2\text{O}_2]} \right)$$

**MAT-II:** The methionine dependence of the MAT-II kinetics is from [13], and we take  $V_{\max} = 289.7 \mu\text{M/hr}$  and  $K_m = 50$ . The inhibition by SAM was derived by non-linear regression on the data from [13], Figure 5. The last factor represents the inhibition of MAT-II by oxidative stress, with  $K_i=35$ , see the discussion above.

$$V_{\text{MATII}} = (0.15 + 0.83e^{-0.0023[\text{SAM}]}) \left( \frac{V_{\max}[\text{Met}]}{K_m + [\text{Met}]} \right) \left( \frac{K_i + [\text{H}_2\text{O}_2]_{\text{SS}}}{K_i + [\text{H}_2\text{O}_2]} \right)$$

**MAT-III.** The methionine dependence of the MAT-III kinetics is from [14], Figure 5, fitted to a Hill equation with  $V_{\max} = 51.52 \mu\text{M/hr}$ ,  $K_m = 300$ . The activation by SAM is from [13], Figure 5, fitted to a Hill equation with  $K_a = 360$ . The last factor represents the inhibition of MAT-III by oxidative stress, with  $K_i=66$ , see the discussion above.

$$V_{\text{MATIII}} = \left( \frac{V_{\max}[\text{Met}]^{1.21}}{K_m + [\text{Met}]^{1.21}} \right) \left( 1 + \frac{7.2[\text{SAM}]^2}{(K_a)^2 + [\text{SAM}]^2} \right) \left( \frac{K_i + [\text{H}_2\text{O}_2]_{\text{SS}}}{K_i + [\text{H}_2\text{O}_2]} \right)$$

**GNMT:** The first term of the GNMT reaction is standard Michaelis-Menten with tissue  $V_{\max} = 226.14$  and liver  $V_{\max} = 364 \mu\text{M/hr}$ , and  $K_m = 63$  [15]. The second term is product inhibition by SAH from [16] with  $K_i = 18$ . The third term, the long-range inhibition of GNMT by folate, was derived by non-linear regression on the data of [17], and scaled so that it equals 1 when the external folate concentration is  $5 \mu\text{M}$  and  $.4 \mu\text{M}$  in the liver and tissue, respectively. The constant A is 5.35 and 0.75 in the liver and tissue, respectively.

$$V_{\text{GNMT}} = \left( \frac{V_{\max}[\text{SAM}]}{K_m + [\text{SAM}]} \right) \left( \frac{1}{1 + \frac{[\text{SAH}]}{K_i}} \right) \left( \frac{A}{0.35 + [\text{Fol}]} \right)$$

**DNMT:** The DNA methylation reaction is given as a uni-reactant scheme with SAM as substrate. That is, the substrates for methylation are assumed constant. Their variation can be modeled by varying the  $V_{\max}$ . The  $V_{\max}$  for the liver and tissue are 120.73 and 66, respectively. Both the liver and tissue have the same  $K_m = 1.4$  and  $K_i = 1.4$ , which is from [18].

$$V_{\text{METH}} = \frac{V_{\text{max}}[\text{SAM}]}{K_m \left(1 + \frac{[\text{SAH}]}{K_i}\right) + [\text{SAM}]}$$

**SAHH:** Both factors of SAHH reaction are standard Michaelis-Menten with positive direction from SAH to Hcy and the negative direction from Hcy to SAH. The kinetic constants for SAH in the liver are  $V_{\text{max,SAH}}=448$ , and  $K_{\text{m,SAH}}= 6.5$  and for the tissue are  $V_{\text{max,SAH}}=320$ , and  $K_{\text{m,SAH}}= 6.5$ . Both the liver and tissue have the same kinetic constants for Hcy, with  $V_{\text{max,Hcy}}= 4530$ , and  $K_{\text{m,Hcy}}= 150$ , and justification for the  $K_{\text{m}}$  values can be found in [12].

$$V_{\text{SAHH}} = \frac{V_{\text{max,SAH}}[\text{SAH}]}{K_{\text{m,SAH}} + [\text{SAH}]} - \frac{V_{\text{max,Hcy}}[\text{Hcy}]}{K_{\text{m,Hcy}} + [\text{Hcy}]}$$

**BHMT:** The kinetics of BHMT are Michaelis-Menten with the parameters  $K_{\text{m}} = 12$ , and  $V_{\text{max}} = 239.3 \mu\text{M/hr}$  [19, 20]. The form of the inhibition of BHMT by SAM was derived by non-linear regression on the data of [21] and scaled so that it equals 1 when the external methionine concentration is  $30 \mu\text{M}$ . The last factor represents the inhibition of BHMT by oxidative stress, see the discussion below.  $K_i = 0.01 \mu\text{M}$  is the inhibition constant.

$$V_{\text{BHMT}} = e^{-(0.0021([\text{SAM}]+[\text{SAH}]))} e^{+(0.0021(71.28))} \left(\frac{V_{\text{max}}[\text{Hcy}]}{K_{\text{m}} + [\text{Hcy}]}\right) \left(\frac{K_i + [\text{H}_2\text{O}_2]_{\text{SS}}}{K_i + [\text{H}_2\text{O}_2]}\right)$$

**MS:** Both factors of MS reaction are standard Michaelis-Menten. The kinetic constants are  $V_{\text{max,Hcy}}=406.25 \mu\text{M/hr}$ ,  $K_{\text{m,Hcy}}= 1 \mu\text{M}$  [22],  $K_{\text{m,FOLATE}}= 25 \mu\text{M}$  [23, 24]. The last factor represents the inhibition of MS by oxidative stress with a  $K_i = 0.01$ , see the discussion below.

$$V_{\text{MS}} = \left(\frac{V_{\text{max}}[\text{Hcy}]}{K_{\text{m,Hcy}} + [\text{Hcy}]}\right) \left(\frac{[\text{Fol}]}{K_{\text{m,FOLATE}} + [\text{Fol}]}\right) \left(\frac{K_i + [\text{H}_2\text{O}_2]_{\text{SS}}}{K_i + [\text{H}_2\text{O}_2]}\right)$$

**CBS:** The kinetics of CBS is standard Michaelis-Menten where the  $V_{\text{max}}$  in the liver and tissue are  $31740 \mu\text{M/hr}$  and  $3174 \mu\text{M/hr}$ , respectively.  $K_{\text{m}} = 1000 \mu\text{M}$  for Hcy and is taken from [25]. The form of the activation of CBS by SAM and SAH was derived by non-linear regression on the data in [26] and [27] scaled so that it equals 1 when the external methionine concentration is  $30 \mu\text{M}$ . The last factor represents the activation of CBS by oxidative stress with  $K_a=0.035$ , see the discussion below.

$$V_{\text{CBS}} = \left(\frac{V_{\text{max}}[\text{Hcy}]}{K_{\text{m}} + [\text{Hcy}]}\right) \left(\frac{(1.2)([\text{SAM}] + [\text{SAH}]^2)}{(30)^2 + ([\text{SAM}] + [\text{SAH}]^2)}\right) \left(\frac{K_a + [\text{H}_2\text{O}_2]}{K_a + [\text{H}_2\text{O}_2]_{\text{SS}}}\right)$$

### Effect of SAM and SAH on 5mTHF

The concentration of 5mTHF depends on the activity of the enzyme MTHFR, which is inhibited by SAM, and this inhibition is counteracted by SAH. Since MTHFR is not present in the current model we used the derivation of the effect of SAM and SAH on 5mTHF described in [28], where the inhibition by SAM is given by the inhibitory factor:

$$I=10/(10+[SAM]-[SAH]) .$$

We introduce a new factor,  $\alpha$ , as the rate of folate input divided by the pre-fortification rate (so  $\alpha=1$  pre-fortification and  $\alpha=1.5$  post-fortification). Using these factors we use the equations from [28] to calculate the dependence of the 5mTHF concentration in the liver on SAM and SAH as

$$5mTHF=35/(((0.0185.*Hcy)/(I*\alpha))-1) .$$

The effect of folate increase is less pronounced in some peripheral tissues than in the liver [29] so we take  $\alpha$  for the tissues to be  $\alpha_t=0.5+(0.5*\alpha)$  and calculate the effect of SAM and SAH on the 5mTHF concentration in the tissue as

$$5mTHF=27/(((0.04.*Hcy)/(I*\alpha_t))-1) .$$

We used these values as the [Fol] terms in the MS and GNMT reactions in the liver and tissue, respectively.

### ***C.3 Transport kinetics***

We now discuss the metabolite transport between compartments. Depending on the metabolite being transported, different kinetic equations were used.

**Met and Hcy transport:** The general formula for Met, and Hcy kinetics transport is taken to be

$$V = \frac{V_{\max}[\text{metabolite}]}{K_m + [\text{metabolite}]}$$

The transport kinetics of a metabolite coming into and out of a compartment is Michaelis-Menten, and the direction of transport is indicated by the subscript of V. For example, the transport of Met from the plasma to liver is notated as  $V_{pMetl}$ , and from the liver to the plasma as  $V_{lMetp}$ . The molecular similarities of Hcy and Met allow for movement into or out of cells by multiple cysteine transport systems [30, 31].  $K_m$  values for Met transport ranges from 2-3000  $\mu\text{M}$  depending on the transport system being used [32], while  $K_m$  for Hcy transport ranges from 19-1000  $\mu\text{M}$  [33]

**SAM and SAH transport:** SAM and SAH transport is taken to be mass action. In accordance with the literature, we assume that SAM and SAH are only exported from cells into the plasma but are not taken up by cells from the plasma [34-36]. The removal of SAM and SAH from the body is thought to occur through urine [37, 38].

**Folate transport:** Transport of folate into and out of a cell occurs through receptor mediated endocytosis, reduced folate-carrier mediated systems, ATP-dependent export and passive diffusion [39].

We use two general formulas for kinetics of folate transport. The first formula is Michaelis-Menten:

$$V = \frac{V_{\max}[\text{pfol}]}{K_m + [\text{pfol}]}$$

The subscript of V indicates the direction of transport. For instance transport of folate from the plasma to the liver is indicated by the notation  $V_{\text{pfol}}$ .  $K_m$  values of folate uptake into cells range from 0.66-0.76  $\mu\text{M}$  [40, 41]. Additionally, the model contains folate flux between compartments, because both the liver and tissue have the ability to import as well as export folate.

The second formula describes the bi-directional diffusive transport of folate between a compartment and plasma:

$$V = d([\text{c1fol}] - [\text{pfol}]),$$

where d is a rate constant describing the flux of folate into and out of a compartment, and c1 indicates the compartment under consideration (liver or peripheral tissue). The subscript of V likewise indicates the relevant compartments. For example, the flux of folate transport into and out of the liver is represented by  $V_{\text{lfluxfol}}$ .

**Table S5. Parameter values for transport kinetics.**

Reaction	Parameter	Model Value	Reaction	Parameter	Model Value
VpHcyl	Km	50	VpMetl	Km	100
	Vmax	8.59		Vmax	406
VlHcyp	Km	50	VlMetp	Km	100
	Vmax	44		Vmax	126
VpHcyt	Km	50	VpMett	Km	100
	Vmax	5.05		Vmax	1600
VtHcyp	Km	50	VtMetp	Km	100
	Vmax	30.62		Vmax	1509.4
VlSAMp	k	0.00095	VlSAHp	k	0.0009
VtSAMp	k	0.0035	VtSAHp	k	0.0007
Vpfol	Km	0.7	Vpfol	Km	0.7
	Vmax	0.094		Vmax	0.043
Vlfluxfol	d	0.000012	Vtfluxfol	d	0.00001

## Part D: Input and Removal Rate of Metabolites

### D1. Input rates ( $\mu\text{M/hr}$ )

**Folate:** After establishing the metabolic kinetics and transport kinetics for each compartment we found that a folate input rate into the plasma compartment of  $0.0024 \mu\text{mol L}^{-1} \text{hr}^{-1}$  established a steady-state concentration of 416 nM in the tissue compartment. This value is close to the observed pre-fortification mean erythrocyte folate concentration corresponding to an estimated average dietary folate intake of about 200  $\mu\text{g/day}$ . When we increased folate input 1.5-fold we obtained a steady-state tissue folate concentration of 622 nM, which matches the mean post-fortification erythrocyte folate concentration, corresponding to an estimated average dietary intake of about 300  $\mu\text{g/day}$ .

**Methionine:** Methionine input in the model is 106  $\mu\text{M}$  per hour.

### D2. Removal Rates ( $\mu\text{M/hr}$ )

The removal of metabolites from a compartment follows the general formula

$$V = k[c_1\text{metabolite}]$$

where  $k$  is a constant that was calculated so that the rate of removal of a metabolite from a compartment accurately reflects experimental data, and  $c_1$  is the compartment the metabolite is currently occupying. The removal of a metabolite is unidirectional and expressed by a linear equation, which is indicated by its transport velocity. For example, the removal of methionine from the plasma is represented by  $V_{\text{pmet}}$ .

A major route of metabolites removal from the body is through filtration of the plasma by the kidney and ultimate loss of the metabolite via urine excretion. Our model does not contain a kidney compartment so loss of a metabolite occurs directly by the removal of the metabolite from the plasma. Additionally, our model assumes that loss of urine is 1L/per 24 hours, which is within the normal range of daily human urine loss [42].

Catabolism by liver and tissue removes most folate from the body, and approximately 1% of folate removal occurs through urine [43]. Our model accounts for folate catabolism in the liver and tissue as well as loss through urine.

**Hcy removal:** We now discuss removal of Hcy from the plasma which is expressed by the formula

$$V = k_{\text{pHcy}}[\text{pHcy}] - \frac{V_{\text{max}}[\text{uHcy}]}{K_m + [\text{uHcy}]}$$

where the prefixes  $p$  and  $u$  stand for the concentration of Hcy in the plasma and the urine. Most Hcy is reabsorbed by the kidney, which allows only 1-2% of it to be removed daily in urine [42, 44]. For the purpose of these calculations we assume that plasma and urine compartments have the same volume and that the transports occur within the kidney tubules and associated capillaries. The kinetics are linear for Hcy going from the plasma and into the urine, with

$k_p\text{Hcy} = 0.73$ . The kinetics is Michaelis-Menten for Hcy going from the urine and back into the plasma, with  $V_{\max} = 0.5$ , and  $K_m = 1$ .

**Table S6. Rate constants for removal of metabolites by catabolism and excretion, and the rate of metabolite loss from the various compartments**

Compartment	Metabolite removed	Removal constant		Rate of removal at steady-state ( $\mu\text{M/hr}$ )		Ref
		name	value ( $\text{hr}^{-1}$ )	model	experiment	
Plasma	Met	kpMet	0.05	1.69	1.7	[45]
	Hcy	kpHcy	0.073	0.14	0.07-0.23	[42]
	SAM	kpSAM	9	0.82	0.42	[38]
	SAH	kpSAH	1.4	0.034	0.02	[38]
	Folate	kpfolate	0.01	0.0001	0.00025	[46]
Liver	Folate	klfolate	0.00027	0.0015		
Tissue	Folate	ktfolate	0.00023	0.0008		

### References

1. Ganji V, Kafai M: **Trends in serum folate, RBC folate, and circulating total homocysteine concentrations in the United States: Analysis of data from National Health and Nutrition Examination Surveys, 1988-1994, 1999-2000, and 2001-2002.** *Journal of Nutrition* 2006, **136**(1):153-158.
2. Loehrer F, Angst C, Brunner F, Haefeli W, Fowler B: **Evidence for disturbed S-adenosylmethionine : S-adenosylhomocysteine ratio in patients with end-stage renal failure: A cause for disturbed methylation reactions?** *Nephrology Dialysis Transplantation* 1998, **13**(3):656-661.
3. Brouwer I, van Dusseldorp M, Duran M, Thomas C, Hautvast J, Eskes T, Steegers-Theunissen R: **Low-dose folic acid supplementation does not influence plasma methionine concentrations in young non-pregnant women.** *British Journal of Nutrition* 1999, **82**(2):85-89.
4. Fowler B: **Transport and Tissue Distribution of Homocysteine and Related S-Adensoyl Compounds.** In: *Homocysteine in Health and Disease*. Edited by Carmel R, Jacobsen D. Cambridge: Cambridge University Press; 2001: 163-175.
5. Hoppner K, Lampi B: **Folate Levels in Human-Liver Autopsies in Canada** *American Journal of Clinical Nutrition* 1980, **33**(4):862-864.
6. Finkelstein J, Kyle W, Harris B, Martin J: **Methionine metabolism in mammals: concentration of metabolites in rat tissues.** *Journal of Nutrition* 1982, **112**(5):1011-1018.
7. Brown R, Delp M, Lindstedt S, Rhomberg L, Beliles R: **Physiological parameter values for physiologically based pharmacokinetic models.** *Toxicology and Industrial Health* 1997, **13**(4):407-484.
8. Deplancke B, Gaskins H: **Redox control of the transsulfuration and glutathione biosynthesis pathways.** *Current Opinion in Clinical Nutrition and Metabolic Care* 2002, **5**(1):85-92.

9. Mosharov E, Cranford M, Banerjee R: **The quantitatively important relationship between homocysteine metabolism and glutathione synthesis by the transsulfuration pathway and its regulation by redox changes.** *Biochemistry* 2000, **39**(42):13005-13011.
10. Corrales F, Ruiz F, Mato J: **In vivo regulation by glutathione of methionine adenosyltransferase S-nitrosylation in rat liver.** *Journal of Hepatology* 1999, **31**(5):887-894.
11. Pajares M, Duran C, Corrales F, Pliego M, Mato J: **Modulation of rat liver S-adenosylmethionine synthetase activity by glutathione.** *Journal of Biological Chemistry* 1992, **267**(25):17598-17605.
12. Reed M, Thomas R, Pavisic J, James S, Ulrich C, Nijhout H: **A mathematical model of glutathione metabolism.** *Theoretical Biology and Medical Modelling* 2008, **5**.
13. Sullivan D, Hoffman J: **Fractionation and kinetic properties of rat liver and kidney methionine adenosyltransferase isozymes.** *Biochemistry* 1983, **22**(7):1636-1641.
14. del Pino M, Corrales F, Mato J: **Hysteretic behavior of methionine adenosyltransferase III - Methionine switches between two conformations of the enzyme with different specific activity.** *Journal of Biological Chemistry* 2000, **275**(31):23476-23482.
15. Ogawa H, Fujioka M: **Purification and properties of glycine N-methyltransferase from rat liver.** *Journal of Biological Chemistry* 1982, **257**(7):3447-3452.
16. Kim D, Huang T, Schirch D, Schirch V: **Properties of tetrahydropteroylpentaglutamate bound to 10-formyltetrahydrofolate dehydrogenase.** *Biochemistry* 1996, **35**(49):15772-15783.
17. Yeo E, Wagner C: **Purification and properties of pancreatic glycine N-methyltransferase.** *Journal of Biological Chemistry* 1992, **267**(34):24669-24674.
18. Flynn J, Reich N: **Murine DNA (Cytosine-5-)-methyltransferase: steady-state and substrate trapping analyses of the kinetic mechanism.** *Biochemistry* 1998, **37**(43):15162-15169.
19. Finkelstein J, Harris B, Kyle W: **Methionine metabolism in mammals: kinetic study of betaine-homocysteine methyltransferase.** *Archives of Biochemistry and Biophysics* 1972, **153**(1):320-324.
20. Skiba W, Taylor M, Wells M, Mangum J, Awad W: **Human hepatic methionine biosynthesis. Purification and characterization of betaine-homocysteine S-methyltransferase.** *Journal of Biological Chemistry* 1982, **257**(24):4944-4948.
21. Finkelstein J, Martin J: **Inactivation of betaine-homocysteine methyltransferase by adenosylmethionine and adenosylethionine.** *Biochemical and Biophysical Research Communications* 1984, **118**(1):14-19.
22. Banerjee R, Chen Z, Gulati S: **Methionine synthase from pig liver.** *Methods in Enzymology* 1997, **281**:189-196.
23. Banerjee R, Frasca V, Ballou D, Matthews R: **Participation of cob(I)alamin in the reaction catalyzed by methionine synthase from Escherichia coli: a steady-state and rapid reaction kinetic analysis** *Biochemistry* 1990, **29**(50):11101-11109.
24. Finkelstein J, Martin J: **Methionine metabolism in mammals. Adaptation to methionine excess.** *Journal of Biological Chemistry* 1986, **261**(4):1582-1587.
25. Finkelstein J: **Regulation of homocysteine metabolism.** In: *Homocysteine in Health and Disease.* Edited by Carmel RJ, D.W. Cambridge: Cambridge Univ. Press; 2001: 92-99.
26. Janosik M, Kery V, Gaustadnes M, Maclean K, Kraus J: **Regulation of human cystathionine beta-synthase by S-adenosyl-L-methionine: evidence for two catalytically active conformations involving an autoinhibitory domain in the C-terminal region.** *Biochemistry* 2001, **40**(35):10625-10633.
27. Kluijtmans L, Boers G, Stevens E, Renier W, Kraus J, Trijbels F, van den Heuvel L, Blom H: **Defective cystathionine beta-synthase regulation by S-adenosylmethionine in a partially pyridoxine responsive homocystinuria patient.** *Journal of Clinical Investigation* 1996, **98**(2):285-289.

28. Nijhout H, Reed M, Anderson D, Mattingly J, James J, Ulrich C: **Long-Range Allosteric Interactions between the Folate and Methionine Cycles Stabilize DNA Methylation Reaction Rate** *Epigenetics* 2006, **1**(2):81-87.
29. Pfeiffer C, Johnson C, Jain R, Yetly E, Picciano M, Rader J, Fisher K, Mulinare J, Osterloh J: **Trends in blood folate and vitamin B-12 concentrations in the United States, 1988-2004.** *American Journal of Clinical Nutrition* 2007, **86**:718-727.
30. Ewadh M, Tudball N, Rose A: **Homocysteine uptake by human umbilical vein endothelial cells in culture.** *Biochimica et Biophysica Acta* 1990, **1054**(3):263-266.
31. Korendyaseva T, Martinove M, Dudchenko A, Vitvitsky V: **Distribution of methionine between cells and incubation medium in suspension of rat hepatocytes.** *Amino Acids* 2010, **39**:1281-1289.
32. Soriano-Garcia J, Torras-Llort M, Ferrer R, Moreto M: **Multiple pathways for L-methionine transport in brush-border membrane vesicles from chicken jejunum.** *Journal of Physiology* 1998, **509**(2):527-539.
33. Budy B, O'Neill R, DiBello P, Sengupta S, Jacobsen D: **Homocysteine transport by human aortic endothelial cells: Identification and properties of import systems.** *Archives of Biochemistry and Biophysics* 2006, **446**(2):119-130.
34. Greenberg M, Chaffee S, Hershfield M: **Basis for resistance to 3-deazaaristeromycin, an inhibitor of S-adenosylhomocysteine hydrolase, in human B-lymphoblasts.** *Journal of Biological Chemistry* 1989, **264**(2):795-803.
35. Hoffman D, Marion D, Cornatzer W, Duerre J: **S-Adenosylmethionine and S-adenosylhomocystein metabolism in isolated rat liver. Effects of L-methionine, L-homocystein, and adenosine.** *Journal of Biological Chemistry* 1980, **255**(22):822-827.
36. Bontemps F, VandenBerghe G: **Metabolism of exogenous S-adenosylmethionine in isolated rat hepatocyte suspensions: methylation of plasma-membrane phospholipids without intracellular uptake.** *Biochemical Journal* 1997, **327**:383-389.
37. Duerre J, Miller C, Reams G: **Metabolism of S-adenosyl-L-homocysteine in vivo by the rat** *Journal of Biological Chemistry* 1969, **244**(1):107-&.
38. Stabler S, Allen R: **Quantification of serum and urinary S-adenosylmethionine and S-adenosylhomocysteine by stable-isotope-dilution liquid chromatography-mass spectrometry.** *Clinical Chemistry* 2004, **50**(2):365-372.
39. Suh J, Herbig A, Stover P: **New perspectives on folate catabolism.** *Annu Rev Nutr* 2001, **21**:255-282.
40. Nabokina S, Ma T, Said H: **Mechanism and regulation of folate uptake by human pancreatic epithelial MIA PaCa-2 cells.** *American Journal of Physiology-Cell Physiology* 2004, **287**(1):C142-C148.
41. Nguyen T, Dyer D, Dunning D, Rubin S, Grant K, Said H: **Human intestinal folate transport: cloning, expression, and distribution of complementary RNA.** *Gastroenterology* 1997, **112**(3):783-791.
42. Chwatko G, Jakubowski H: **Urinary excretion of homocysteine-thiolactone in humans.** *Clinical Chemistry* 2005, **51**(2):408-415.
43. InsituteofMedicine: **Dietary reference intake.** Washington, DC: National Academy Press; 1998.
44. Refsum H, Helland S, Ueland P: **Radioenzymic determination of homocysteine in plasma and urine.** *Clinical Chemistry* 1985, **31**:624-628.
45. Stipanuk M: **Sulfur amino acid metabolism: pathways for production and removal of homocysteine and cysteine.** *Annu Rev Nutr* 2004, **24**:539-577.

46. Gregory J, Williamson J, Bailey L, Toth J: **Urinary excretion of H-2(4) folate by nonpregnant women following a single oral dose of H-2(4) folic acid is a functional index of folate nutritional status.** *Journal of Nutrition* 1998, **128**(11):1907-1912.